Computational Fluid Dynamics (CFD) Simulation and Comparison for Different Numbers of Baffles to Reduce Concentration Polarization Effects in Membrane Tubes

Muhammad Ahsan* **& Arshad Hussain**

School of Chemical and Materials Engineering (SCME), National University of Sciences and Technology (NUST), Islamabad, Pakistan
*E-mail: ahsan@scme.nust.edu.pk

Abstract. This research shows the use of computational fluid dynamics (CFD) with finite volume method (FVM) to study the species diffusion and mixing characteristics in a tubular membrane filled with vertical baffles. This study exhibits how to set up the FVM for CFD simulation and residence time distribution (RTD) analysis and compare the mixing characteristics of two membrane tubes with a different number of baffles using RTD curves. In this study, the effects of the number of baffles on flow patterns, features and behavior of air were identified completely through computational fluid dynamics (CFD) simulations. In addition, a two-dimensional simulation was implemented to study the effects of steady and unsteady (transient) flow in the tubular membrane. The residence time distribution (RTD) of a tracer in a co-current flow pattern was investigated. For this, the tracer was injected for 1 second into the membrane tubes on a frozen flow field and the concentration variation of the tracer over time was monitored at the outlet.

Keywords: *computational fluid dynamics; residence time distribution; tubular membrane; turbulent flow; vertical baffles.*

1 Introduction

Concentration polarization decreases permeation in the gas separation process [1]. Turbulence promoters are normally applied to overcome this unwanted phenomenon [2]. They are also applied to increase the efficiency of the membrane [3]. For this purpose, several researchers have proposed geometric conditions for different membrane processes [4].

In these studies, it has been established that installation of baffles should be modest and active to enhance permeation of a specific gas [5,6]. Different orientations and shapes of baffles have been used in other studies [7,8]. Mass transfer in a baffle-filled membrane tube is a complex phenomenon for which several experimental investigations are available in the literature [9-12]. By mathematically modeling the flow of fluid in membrane tubes equipped with baffles, the wall concentration and local flux by mass balance have been studied

Received July 4th, 2016, Revised January 16th, 2017, Accepted for publication March 20th, 2017.
Copyright ©2017 Published by ITB Journal Publisher, ISSN: 2337-5779, DOI: 10.5614/j.eng.technol.sci.2017.49.1.7

[13-15]. Numerical methods with great precision, such as computational fluid dynamics (CFD), have been developed and established in the last decade [16,17].

Liu, *et al.* [18] used mixing-promoting baffles to simulate the mass transfer in a slit membrane tube for an effective elimination of volatile organic compounds. Santos, *et al.* [19] developed a mathematical simulation of membrane tubes filled with flow-aligned spacers. They established that mass transfer effectiveness and friction should play an important role in the selection of the finest spacer. The effects of different spacers on flow behavior has been studied by applying CFD software in annular and flat channels [20]. The results of the simulation showed that there is no significant change in the fluid flow in a flat-channel and spacer-filled spiral configuration. The membrane flux is raised considerably by using baffles in the tube. The qualitative and quantitative properties of the fluid flow in a membrane tube filled with baffles still require more research [21,22].

In the present research, a 2D perpendicular baffle-filled membrane tube was used to simulate a turbulent flow using finite volume solver ANSYS FLUENT® to examine the effect of changing the number of baffles on the flow pattern. Additionally, the distribution of velocity, the turbulence characteristic and mass concentration were considered. Mass concentration in the membrane tube was studied for the residence time distribution analysis to predict a better design. The results obtained for different numbers of baffles were compared first to reduce concentration polarization effects in the membrane tube.

2 CFD Model Formulation and Simulation Setup

For designing a steady state well-mixed module, it is necessary to analyze the flow characteristics of different membrane tubes filled with baffles and compare the RTDs. In this study, a tracer was injected for 1 second into membrane tubes on a frozen flow field and the concentration variation of the tracer with time was monitored at the outlet. The schematics of the two models used are shown in Figure 1. The first model had 5 baffles, while the second model had 15 baffles. All the other design parameters were the same in both cases. The flow was turbulent and the inlet fluid had a velocity of 0.5 m/s (Reynolds number = 27383).

The meshes of the two models are shown in Figure 2. The mesh was created using GAMBIT® with the quad meshing scheme. Mesh analysis was carried out using three different mesh intervals, i.e. 1 mm, 2 mm, and 3 mm. The results of the different simulations showed no major differences. The mesh had been

developed with a minimum orthogonal quality of 9.99×10^{-1}. The mesh had one partition with 51800 cells, 105532 faces and 53718 nodes [23].

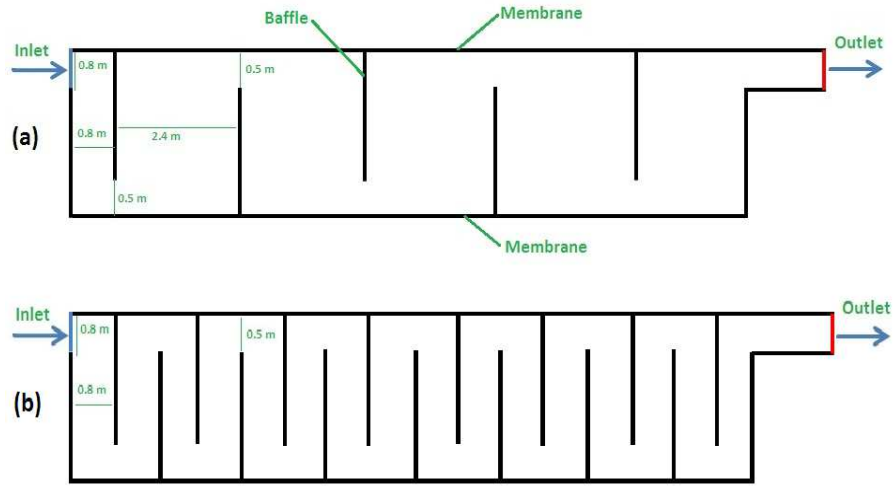

Figure 1 Membrane tubes filled with baffles: (a) 5 baffles (b) 15 baffles.

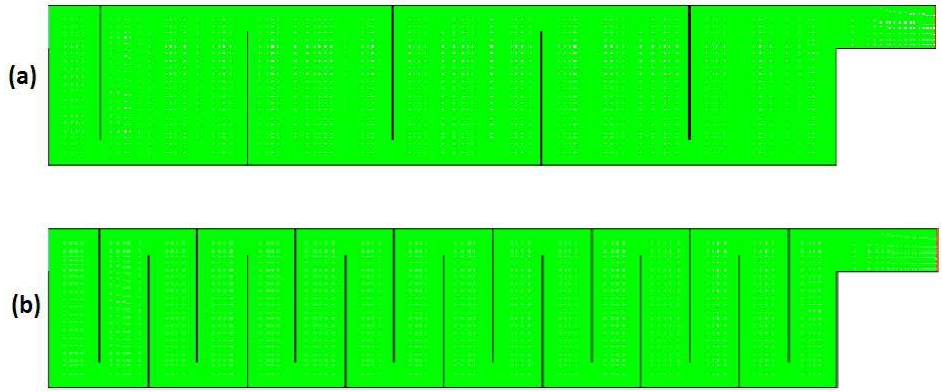

Figure 2 Mesh display: (a) 5 baffles (b) 15 baffles.

The continuity equation in differential form is defined by Eq. (1):

$$\frac{\partial \rho}{\partial t} + \nabla.(\rho\vec{v}) = 0 \tag{1}$$

Conservation of momentum is defined by Eq. (2):

$$\frac{\partial}{\partial t}(\rho\vec{v}) + \nabla.(\rho\vec{v}\vec{v}) = -\nabla \mathrm{p} + \nabla.(\bar{\bar{\tau}}) + \rho\vec{g} + \vec{F} \tag{2}$$

The two-equations model is the most simple and best-known turbulence model. In this model, the turbulent length scales and velocity are calculated independently by using the solutions of different transport equations. The standard k-ϵ model has become the most widely used turbulence model for the solution of practical engineering flow problems [24,25].

The transport equations for the Standard k-ϵ Model are expressed in Eqs. (3) and (4):

$$\frac{\partial}{\partial t}(\rho k) + \frac{\partial}{\partial x_i}(\rho k u_i) = \frac{\partial}{\partial x_j}\left[\left(\mu + \frac{\mu_t}{\sigma_k}\right)\frac{\partial k}{\partial x_j}\right] + G_k + G_b - \rho\epsilon - Y_M + S_k \tag{3}$$

and

$$\frac{\partial}{\partial t}(\rho\epsilon) + \frac{\partial}{\partial x_i}(\rho\epsilon u_i) =$$
$$\frac{\partial}{\partial x_j}\left[\left(\mu + \frac{\mu_t}{\sigma_\epsilon}\right)\frac{\partial \epsilon}{\partial x_j}\right] + C_{1\epsilon}\frac{\epsilon}{k}(G_k + C_{3\epsilon}G_b) - C_{2\epsilon}\rho\frac{\epsilon^2}{k} + S_\epsilon \tag{4}$$

The equation of the turbulent viscosity is defined by Eq. (5):

$$\mu_t = \rho C_\mu \frac{k^2}{\epsilon} \tag{5}$$

The model constants are:

$C_{1\epsilon} = 1.44$, $C_{2\epsilon} = 1.92$, $C_\mu = 0.09$, $\sigma_k = 1.0$, $\sigma_\epsilon = 1.3$

For a turbulent flow, Fick's law in Eqs. (6) to (9) is used to calculate the diffusion flux of a chemical species:

$$J_i = -\left(\rho D_{i,m} + \frac{\mu_t}{Sc_t}\right)\nabla Y_i - D_{T,i}\frac{\nabla T}{T} \tag{6}$$

$$D_{i,m} = \frac{1 - X_i}{\sum_{j,j\neq i}(X_j/D_{ij})} \tag{7}$$

$$Sc_t = \frac{\mu_t}{\rho D_t} \tag{8}$$

$$\frac{\partial}{\partial t}(\rho Y_i) + \nabla.(\rho\vec{v}Y_i) = -\nabla.\vec{J_i} + R_i + S_i \tag{9}$$

The external time distribution can be calculated by Eq.(10):

$$E(t) = \frac{C(t)}{\int_0^\infty C(t)dt} \tag{10}$$

Here $C(t)$ is the concentration of tracer at the outlet as a function of time. $\int_0^\infty C(t)dt$ represents the fraction of species that spend a time less than t inside the membrane tube.

The fraction of species that spend a time more than t is calculated by Eq. (11):

$$F(t) = 1 - \int_0^t E(t)dt \tag{11}$$

Table 1 shows the properties of air and their values used in this study. In this research, it was assumed that the fluid is under turbulent flow with Newtonian, isothermal, incompressible, and constant physical properties. Table 2 shows the boundary conditions used for the CFD simulation.

Table 1 Values of different air properties used in CFD modeling.

Property	Unit	Value
Density	Kg/m^3	1.225
Specific heat	j/kg-k	1006.43
Thermal conductivity	w/m-k	0.0242
Molecular weight	kg/kg-mole	28.966
Viscosity	kg/m-s	1.72×10^{-5}
Mass diffusivity	m^2/s	2.88×10^{-5}

Table 2 Boundary conditions at Inlet for CFD simulation.

Property	Unit	Value
Velocity magnitude	m/s	0.5
Turbulent intensity	%	5
Hydraulic diameter	m	0.8

Figure 3 illustrates the solution procedure for steady and unsteady (transient) problems. In this model, the SIMPLE algorithm is used for pressure-velocity coupling. This algorithm is based on the predictor-corrector approach. The least squares cell-based approach is applied for the evaluation of gradients.

The PRESTO scheme is used for pressure discretization due to flows within strongly curved domains. The second order upwind scheme solves spatial discretization of momentum. The first order scheme is applied for the discretization of both the turbulent kinetic energy and the turbulent dissipation rate. An Intel Core i5 with 4GB RAM was used to solve the steady and unsteady problem.

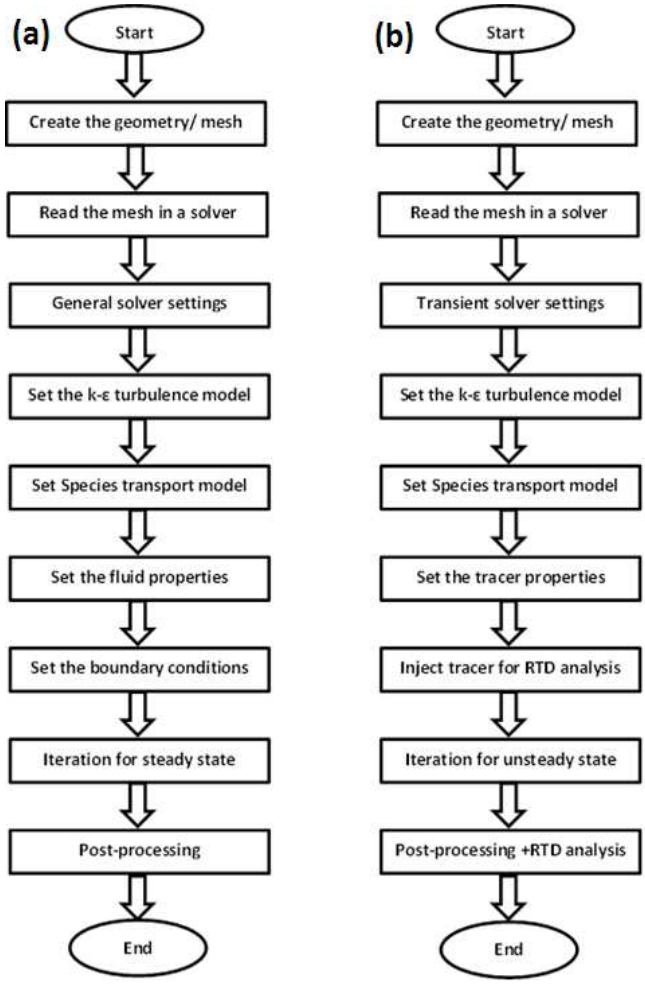

Figure 3 Solution procedure for (a) steady state and (b) unsteady state problems.

3 Results and Discussion

3.1 Velocity Contours

The turbulent flow in a baffle-filled membrane tube was simulated by applying the CFD method. For comparison, the fluid flow in an empty tube was also simulated. Figure 4 shows the contours of the velocity in the membrane tube filled with baffles. At an inlet velocity of 0.5 m/s, the fluid flow is completely turbulent in the bulk stream. Laminar flow layers also occur close to the lower and upper membrane wall, where the fluid velocity is minimal. The species in

the feed stream are concentrated on a specific small area of the membrane surface forming a thick layer, which results in the drop of permeation flux.

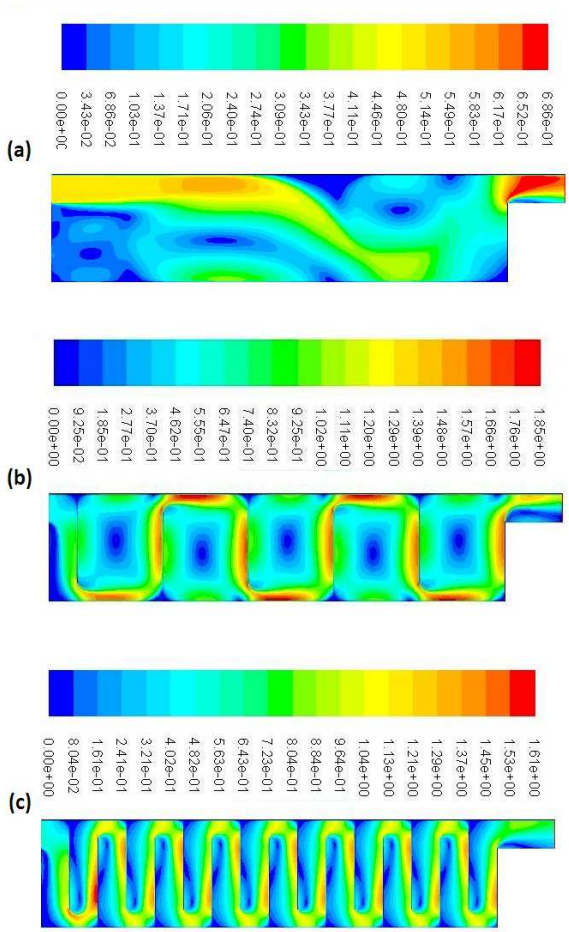

Figure 4 Contours of velocity magnitude (m/s) for membrane tubes (a) without baffles, (b) 5 baffles, (c) 15 baffles.

The presence of a series of baffles increases the turbulence in the fluid stream. The above effects are likely to minimize the concentration polarization and thus increase the membrane's efficiency. A central zone appears before each baffle in the 5-baffle membrane tube, where the velocity is minimal. This does not influence the permeation flux in the membrane tube. The large low-velocity zones are not adjacent to the membrane; the fluid touches the membrane surface in large areas, so a significant increase in the permeation flux is achieved. This approach can clarify why the baffle-filled tubes reached a higher permeation

flux than the empty membrane tube. It was visibly established that the tube with 5 baffles provided a higher membrane surface than the one with 10 baffles. For the 5-baffle case, the velocity behavior differed marginally from the 15-baffle case. The highest velocity occurred in the center of each vertical baffle as well as on the membrane surface next to each baffle. Hence, the membrane tube with 5 baffles is predicted to provide a better permeation flux.

3.2 Velocity Convergence

The convergence histories of velocity magnitude in three membrane tubes (without baffles, with 5 baffles, and with 15 baffles) against iteration are shown in Figure 5. It can be observed that the velocity magnitude in the membrane tube without baffles achieved the highest peak value when compared to the other two tubes.

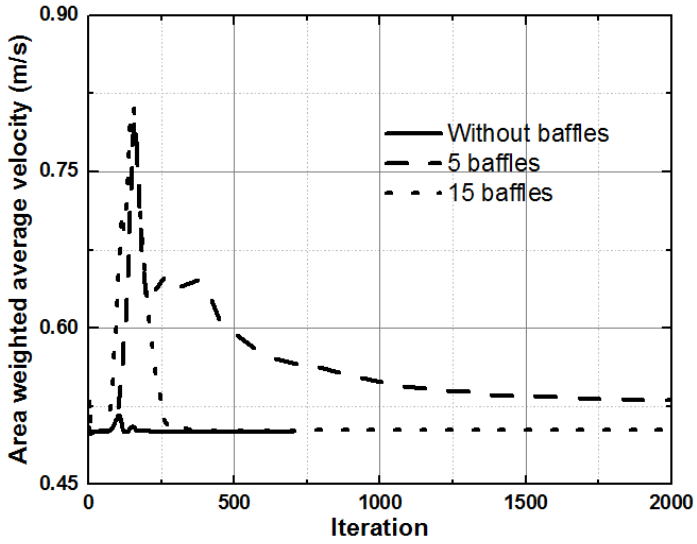

Figure 5 Convergence history of velocity magnitude.

Fluctuation is not sufficient in the empty membrane tube. In the 5- and 15-baffle cases, we can see that the peak values were attained after 150 iterations. At the start, the fluid flows at the inlet velocity before reaching the first baffle, after which it sharply increases its velocity and reaches its peak value. In the 15-baffle case, after reaching peak value, the fluid velocity radically drops to its initial value. However, in the 5-baffle case, the velocity remains above the initial value. At an inlet velocity of 0.5 m/s, the base and peak values of velocity were about 0.5 and 0.8 m/s, respectively. It has been generally verified that the

maximum velocity at the membrane wall can efficiently decrease the species concentration on the membrane surfaces, thus increasing the permeation flux.

3.3 Contours of Tracer Concentration

For the RTD analysis, a fluid called 'tracer' was injected into the membrane tubes for 1 second. This fluid has the same properties as air. The transient simulation was completed using the tracer as a material in FVM. The frozen flow field was selected to avoid the effect of the tracer on the bulk fluid. After the 1-second injection, the tracer was stopped and the simulation was run further to analyze the RTD of the membrane tube. The concentration of injected tracer for the without-baffle case is shown in Figure 6(a). In Figure 6(b) we can observe the concentration after 2000 time steps. The size of each time step was 0.1.

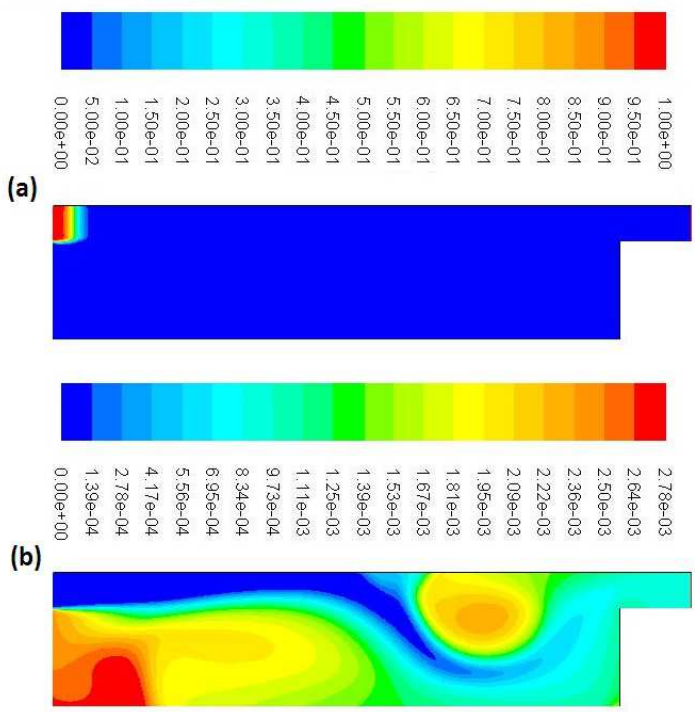

Figure 6 Contours of mass fraction of tracer for membrane tube without baffles (a) after 1 second of injection and (b) after 2000 time steps.

The concentration of tracer at the outlet as a function of time after 1 second for the 5-baffle case is shown in Figure 7(a). There was still a finite concentration of tracer at the outlet after 2000 time steps, as shown in Figure 7(b). The

unsteady run was continued for 2500 more time steps. The concentration of tracer at the outlet as a function of time after 4500 time steps is shown in Figure 7(c). Figure 8(a) shows the mass concentration of injected tracer after 1 second for the 15-baffle case. The mass-weighted average of tracer concentration was negligibly small after 200 time steps, as shown in Figure 8(b). Hence, the data were sufficient to conduct the RTD analysis.

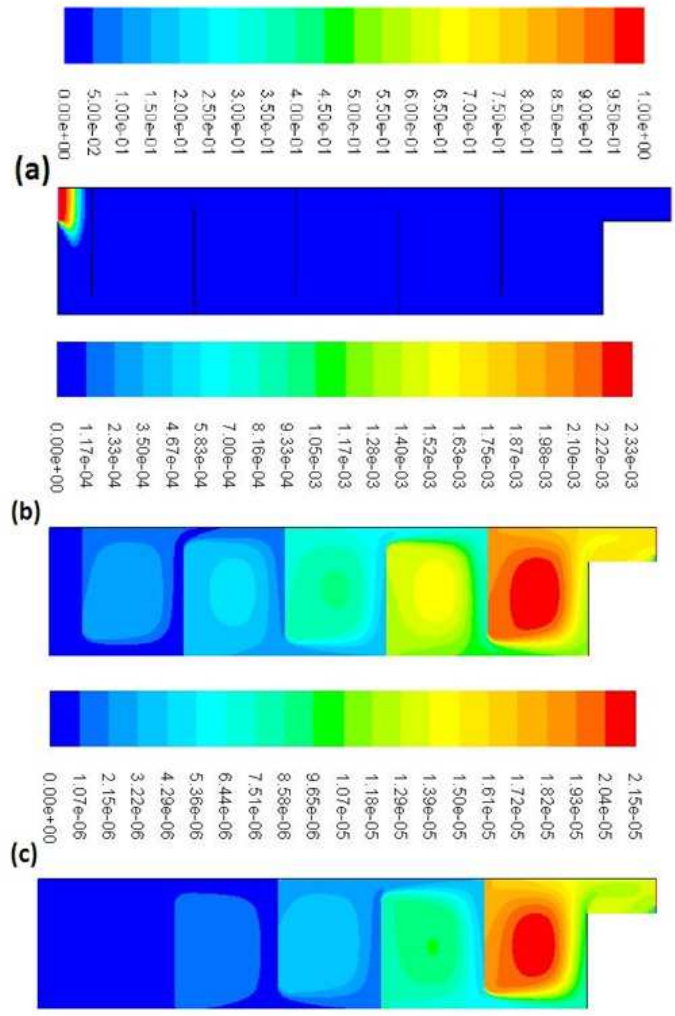

Figure 7 Contours of mass fraction of tracer for membrane tube with 5 baffles (a) after 1 second of injection, b) after 2000 time steps, and (c) after 4500 time steps.

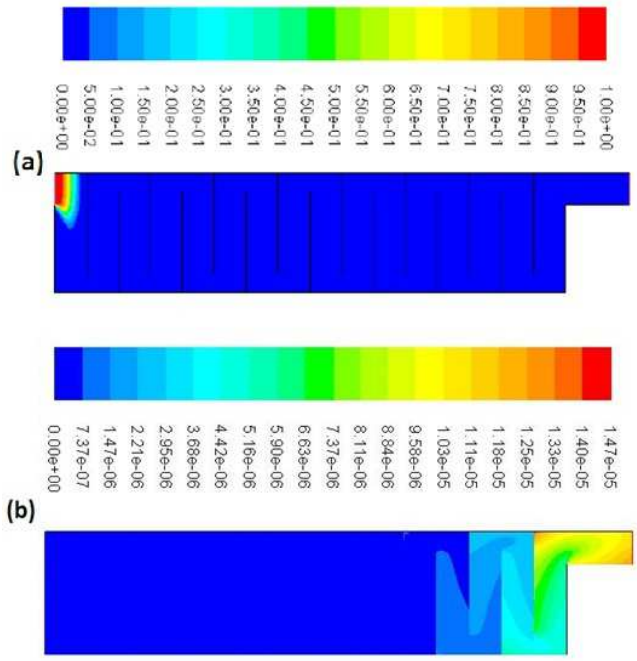

Figure 8 Contours of mass fraction of tracer for membrane tube with 15 baffles (a) after 1 second of injection and (b) after 2000 time steps.

3.4 Residence Time Distribution (RTD) Analysis

Figures 9-11 show the concentration of tracer for the without-baffles, 5-baffles, and 15-baffle cases respectively. In the mass weighted average profiles for the without-baffle and 15-baffle cases we get parabolic curves. We can observe the minimum value on both sides of the parabola for both cases. The behavior of the curve for the concentration in the 5-baffle case was different from the other two. Figure 10 shows a sharp increase in the fluctuation of concentration followed by a long tail. Figures 12-14 show the E-curves of all the cases. The concentration values were multiplied with delta-t, which is 0.1. All the values of this concentration at the various times were added to get the denominator of the equation for external time distribution, E(t) in Equation 10. Applying Equation 10, the ratio between the concentration at each time step and the sum of the product of concentration with delta-t were taken to get the RTD (E-curve). As can be seen from this figure, the general trend of the observed RTDs for the without-baffle and the 15-baffle cases were quite similar. The trend of RTD for the 5-baffle case was different due to the size of the gap between the baffles. This gap influences the RTD behavior in the membrane tube with 5 baffles. Comparing all cases, the highest RTD value was achieved in the 15-baffle case and the lowest RTD value in the 5-baffle case.

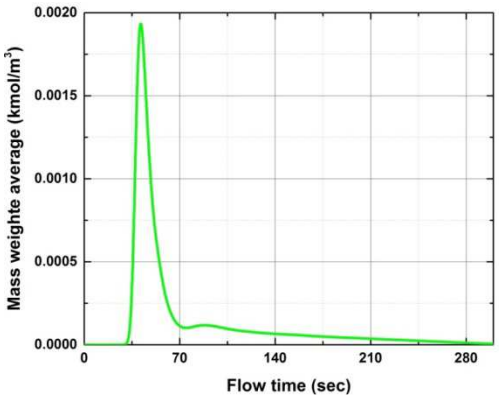

Figure 9 Concentration of tracer over time for without-baffle case.

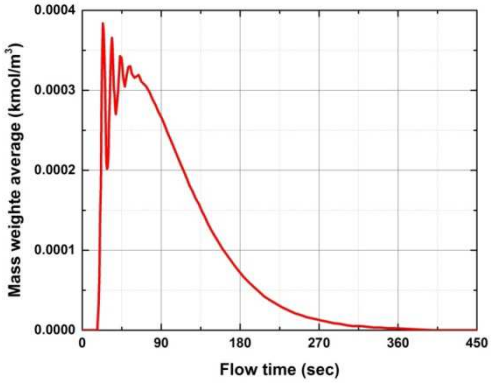

Figure 10 Concentration of tracer over time for 5-baffle case.

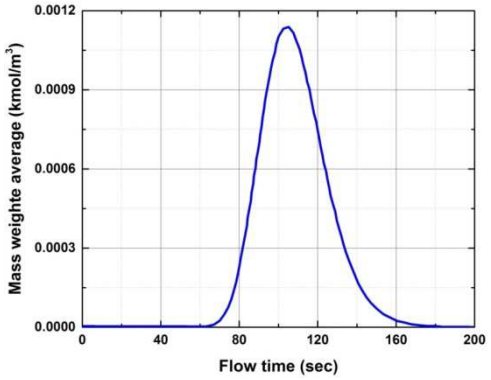

Figure 11 Concentration of tracer over time for 15 baffle case.

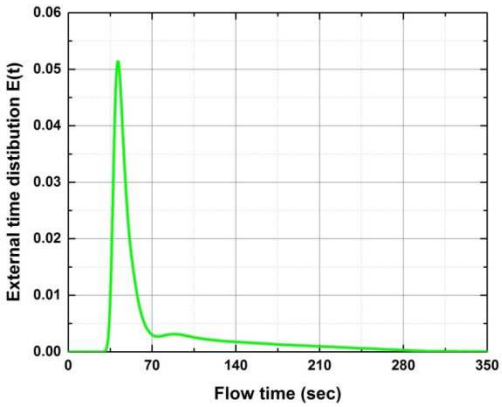

Figure 12 E-curve for membrane without baffles.

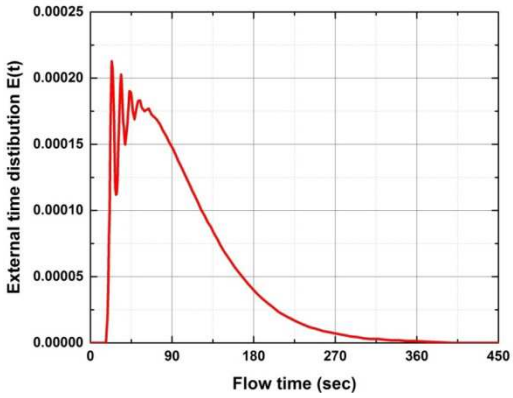

Figure 13 E-curve for membrane with 5 baffles.

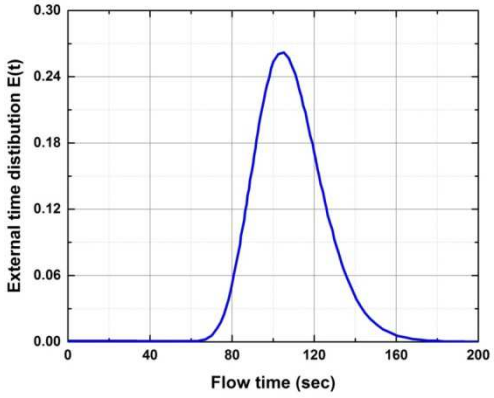

Figure 14 E-curve for membrane tube with 15 baffles.

Table 3 shows the residence time comparison, which is helpful for selecting a suitable design of the membrane tube based on the requirements. Equation 11 was used to calculate the minimum time for which 75%, 50% and 25% of species reside inside the tube.

Table 3 Residence time comparison for three cases.

Species (%) inside membrane tube	75%	50%	25%
Time (s) for case without baffles	41.70	47.70	72.60
Time (s) for case with 5 baffles	25.05	35.20	58.40
Time (s) for case with 15 baffles	91.80	102.50	117.30

3.5 Contours of Pressure Drop and Turbulence Dissipation Rate

Figure 15 shows the pressure drop in the membrane tubes with 5 and 15 baffles respectively. The pressure drop along the tubes can be observed clearly. The pressure drop increases with the increase in the number of baffles in the tube.

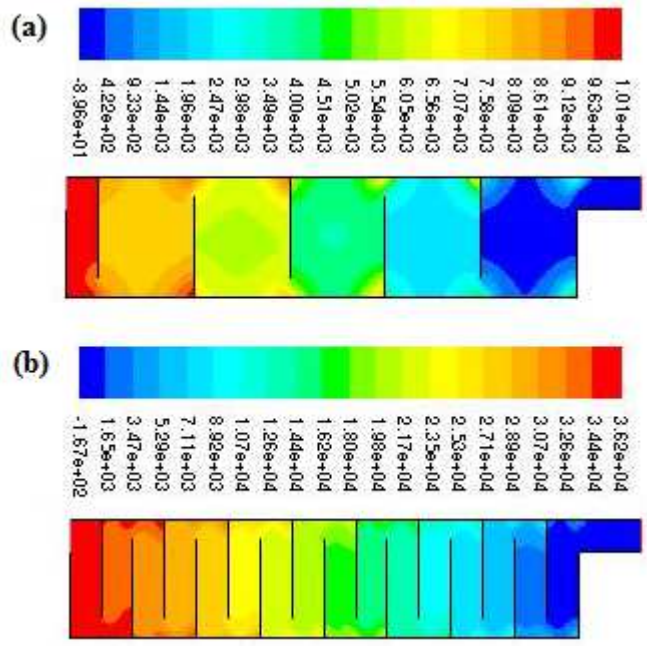

Figure 15 Contours of pressure drop (pascal) for (a) 5 baffles and (b) 15 baffles.

Figure 16 shows the turbulence dissipation rate in the membrane tubes with 5 and 15 baffles respectively. The conversion of turbulence kinetic energy into

thermal energy can be observed in the tubes with 5 and 15 baffles respectively. The turbulence dissipation rate was higher in the tube with 15 baffles.

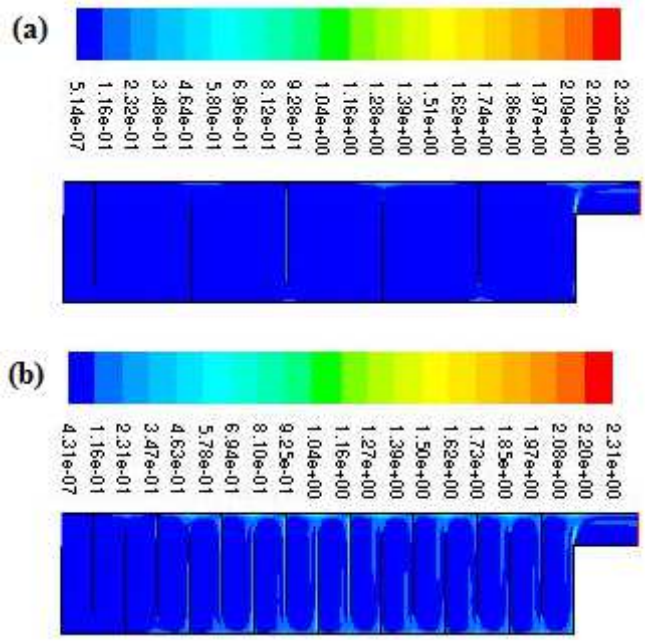

Figure 16 Contours of turbulence dissipation rate (m^2/s^3) for (a) 5 baffles and (b) 15 baffles.

4 Conclusions

In this work, turbulent flow was simulated in baffle-filled membrane tubes using the CFD technique to investigate the flow pattern and velocity magnitude in detail. It was observed that the turbulence generated by the presence of baffles in the membrane tubes was helpful in increasing the contact between the membrane surface and the fluid. This is helpful in reducing the concentration polarization and increasing the permeation flux. A membrane tube with 5 baffles is predicted to provide better permeation flux than a membrane tube with 15 baffles and the empty membrane tube. It was observed that a regular change in flow path may create eddies before each baffle. This could increase the pressure loss and energy cost because of the energy dissipation in the turbulent flow. Therefore, the design of a membrane system filled with baffles contains a trade-off between different competing effects. Moreover, an RTD analysis was implemented by receiving the response of a tracer injected into the three different types of membranes.

Nomenclature

ρ = Fluid density
t = Time
$\vec{v}$ = Flow velocity vector field
P = Static pressure
$\bar{\bar{\tau}}$ = Stress tensor
$\rho\vec{g}$ = Gravitational body force
$\vec{F}$ = External body forces
Gk = Generation of turbulence kinetic energy due to the mean velocity gradients
Gb = Generation of turbulence kinetic energy due to buoyancy
YM = Contribution of the fluctuating dilatation incompressible turbulence to the overall dissipation rate
$C_{1\epsilon}$, $C_{2\epsilon}$,$C_{3\epsilon}$ = Constants
σ_k = Turbulent Prandtl number for k
σ_ϵ = Turbulent Prandtl numbers ϵ, respectively
S_k, S_ϵ = User-defined source terms
μ_t = Turbulent (or eddy) viscosity
C_μ = Constant
$D_{i,m}$ = Mass diffusion coefficient for species i in the mixture
$D_{T,i}$ = Thermal diffusion coefficient
$D_{i,m}$ = Can be specified in a variety of ways, including by specifying the binary mass diffusion coefficient of component i in component j ($D_{i,j}$)
X_i = Mole fraction of species i
Sc_t = Effective Schmidt number for the turbulent flow
D_t = Effective mass diffusion coefficient due to turbulence
Y_i = Local mass fraction of each species
R_i = Net rate of production of species i
S_i = Rate of creation by addition from the dispersed phase

References

[1] Howell, J.A., Field, R.W. & Wu, D., *Yeast Cell Microfiltration: Flux Enhancement in Baffled and Pulsatile Flow Systems*, Journal of Membrane Science, **80**, pp. 59-72, 1993.

[2] Bellhouse, B.J., Costigan, G., Abhinava, K. & Merry, A., *The Performance of Helical Screw Thread Inserts in Tubular Membranes*, Separation, and Purification Technology, **22-23**, pp. 89-113, 2001.

[3] Krstić, D.M., Tekić, M.N., Carić, M.Đ. & Milanović, S.D., *The Effect of Turbulence Promoter on Cross-Flow Microfiltration of Skim Milk*, Journal of Membrane Science, **208**(1-2), pp. 303-314, 2002.

[4] Xu, N., Xing, W., Xu, N. & Shi, J., *Application of Turbulence Promoters in Ceramic Membrane Bioreactor Used for Municipal Wastewater Reclamation,* Journal of Membrane Science, **210**(2), pp. 307-313, 2002.

[5] Neal, P.R., Li, H., Fane, A.G. & Wiley, D.E., *The Effect of Filament Orientation on Critical Flux and Particle Deposition in Spacer-filled Channels,* Journal of Membrane Science, 214(2), pp. 165-178, 2003.

[6] Hussain, A., Nasir, H. & Ahsan, M., *Process Design Analyses of CO_2 Capture from Natural Gas by Polymer Membrane*, Journal of The Chemical Society of Pakistan, **36**(3), pp.411-421, 2014.

[7] Hwang, J.J. & Liou, T.M., *Heat Transfer and Friction in a Low-Aspect-Ratio Rectangular Channel with Staggered Perforated Ribs on Two Opposite Walls*, Journal of Heat Transfer, **117**(4), pp. 843-850, 1995.

[8] Tandiroglu, A., *Effect of Flow Geometry Parameters on Transient Heat Transfer for Turbulent Flow in a Circular Tube with Baffle Inserts*, International Journal of Heat and Mass Transfer, **49**(9-10), pp. 1559-1567, 2006.

[9] Finnigan, S.M. & Howell, J.A., *Effect of Pulsatile Flow On Ultrafiltration Fluxes in A Baffled Tubular Membrane System*, Chemical Engineering Research and Design, **67**(3), pp. 278-282, 1989.

[10] Mackley, M.R., Tweddle, G.M. & Wyatt, I.D*., Experimental Heat Transfer Measurements for Pulsatile Flow in Baffled Tube*s, Chemical Engineering Science, **45**(5), pp. 1237-1242, 1990.

[11] Mackay, M.E., Mackley, M.R. & Wang, Y., *Oscillatory Flow within Tubes Containing Wall or Central Baffles*, Chemical Engineering Research and Design, **69**(6), pp. 506-513, 1991.

[12] Brunold, C.R., Hunns, J.C.B., Mackley, M.R. & Thompson, J.W., *Experimental Observations on Flow Patterns and Energy Losses for Oscillatory Flow in Ducts Containing Sharp Edges*, Chemical Engineering Science, **44**(5), pp. 1227-1244, 1989.

[13] Wang, Y., Howell, J.A., Field, R.W. & Wu, D., *Simulation of Cross-Flow Filtration for Baffled Tubular Channels and Pulsatile Flow*, Journal of Membrane Science, **95**(3), pp. 243-258, 1994.

[14] Chiu, T.Y. & James, A.E*. Effects of Axial Baffles In Non-Circular Multi-Channel Ceramic Membranes using Organic Feed*, Separation and Purification Technology, **51**(3), pp. 233-239, 2006.

[15] Xie, F., Chen, W., Wang, J. & Liu, J., *CFD And Experimental Studies on the Hydrodynamic Performance of Submerged Flat-Sheet Membrane Bioreactor Equipped with Micro-Channel Turbulence Promoters,* Chemical Engineering and Processing: Process Intensification, **99**, pp. 72-79, 2016.

[16] Ahsan, M. & Hussain, A., *Computational Fluid Dynamics (CFD) Modeling of Heat Transfer in a Polymeric Membrane using Finite Volume Method*, Journal of Thermal Science, **22**(6), pp. 564-570, 2016.
[17] Ahsan, M. & Hussain, A., *Mathematical Modeling of Membrane Gas Separation using Finite Difference Method*, Pacific Science Review A: Natural Science and Engineering, **18** (1), pp. 47-52, 2016.
[18] Liu, S.X., Peng, M. & Vane, L.M., *CFD Simulation of Effect of Baffle on Mass Transfer in a Slit-Type Pervaporation Module*, Journal of Membrane Science, **265**(1-2), pp. 124-136, 2005.
[19] Santos, J.L.C., Geraldes, V., Velizarov, S. & Crespo, J.G., *Investigation of Flow Patterns and Mass Transfer in Membrane Module Channels Filled with Flow-Aligned Spacers Using Computational Fluid Dynamics (CFD),* Journal of Membrane Science, **305**(1-2), pp. 103-117, 2007.
[20] Ranade, V.V. & Kumar, A., *Comparison of Flow Structures in Spacer-Filled Flat and Annular Channels,* Desalination, **191**(1-3), pp. 236-244, 2006.
[21] Liu, Y., He, G., Liu, X., Xiao, G. & Li, B., *CFD Simulations of Turbulent Flow in Baffle-Filled Membrane Tube*s, Separation and Purification Technology, **67**(1), pp. 14-20, 2009.
[22] Liu, Y., He, G., Tan, M., Nie, F. & Li, B., *Artificial Neural Network Model for Turbulence Promoter-Assisted Crossflow Microfiltration of Particulate Suspensions,* Desalination, **338**(1), pp. 57-64, 2014.
[23] Fluent, A., ANSYS Fluent 13 Tutorial Guides, Fluent Inc., 2010.
[24] Rolander, N., Rambo, J., Joshi, Y., Allen, J.K. & Mistree, F., *An Approach to Robust Design of Turbulent Convective Systems*, Journal of Mechanical Design, **128**(4), pp. 844-855, 2006.
[25] Fluent, A., Fluent 6.3 User Guides: 8.9.1 Fickian Diffusion, Fluent Inc., pp. 65-66, 2006.